

University of Groningen

Elevated VMP1 expression in acute myeloid leukemia amplifies autophagy and is protective against venetoclax-induced apoptosis

Folkerts, Hendrik; Wierenga, Albertus T; van den Heuvel, Fiona A; Woldhuis, Roy R; Kluit, Darlyne S; Jaques, Jennifer; Schuringa, Jan Jacob; Vellenga, Edo

Published in:
Cell death & disease

DOI:
[10.1038/s41419-019-1648-4](https://doi.org/10.1038/s41419-019-1648-4)

IMPORTANT NOTE: You are advised to consult the publisher's version (publisher's PDF) if you wish to cite from it. Please check the document version below.

Document Version
Publisher's PDF, also known as Version of record

Publication date:
2019

[Link to publication in University of Groningen/UMCG research database](#)

Citation for published version (APA):

Folkerts, H., Wierenga, A. T., van den Heuvel, F. A., Woldhuis, R. R., Kluit, D. S., Jaques, J., Schuringa, J. J., & Vellenga, E. (2019). Elevated VMP1 expression in acute myeloid leukemia amplifies autophagy and is protective against venetoclax-induced apoptosis. *Cell death & disease*, 10(6), [421].
<https://doi.org/10.1038/s41419-019-1648-4>

Copyright

Other than for strictly personal use, it is not permitted to download or to forward/distribute the text or part of it without the consent of the author(s) and/or copyright holder(s), unless the work is under an open content license (like Creative Commons).

The publication may also be distributed here under the terms of Article 25fa of the Dutch Copyright Act, indicated by the "Taverne" license. More information can be found on the University of Groningen website: <https://www.rug.nl/library/open-access/self-archiving-pure/taverne-amendment>.

Take-down policy


If you believe that this document breaches copyright please contact us providing details, and we will remove access to the work immediately and investigate your claim.

Downloaded from the University of Groningen/UMCG research database (Pure): <http://www.rug.nl/research/portal>. For technical reasons the number of authors shown on this cover page is limited to 10 maximum.

ARTICLE

Open Access

Elevated VMP1 expression in acute myeloid leukemia amplifies autophagy and is protective against venetoclax-induced apoptosis

Hendrik Folkerts¹, Albertus T. Wierenga^{1,2}, Fiona A. van den Heuvel^{1,2}, Roy R. Woldhuis¹, Darlyne S. Kluit¹, Jennifer Jaques¹, Jan Jacob Schuringa¹  and Edo Vellenga¹

Abstract

Vacuole membrane protein (VMP1) is a putative autophagy protein, which together with Beclin-1 acts as a molecular switch in activating autophagy. In the present study the role of VMP1 was analysed in CD34⁺ cells of cord blood (CB) and primary acute myeloid leukemia (AML) cells and cell lines. An increased expression of VMP1 was observed in a subset of AML patients. Functional studies in normal CB CD34⁺ cells indicated that inhibiting VMP1 expression reduced autophagic-flux, coinciding with reduced expansion of hematopoietic stem and progenitor cells (HSPC), delayed differentiation, increased apoptosis and impaired *in vivo* engraftment. Comparable results were observed in leukemic cell lines and primary AML CD34⁺ cells. Ultrastructural analysis indicated that leukemic cells overexpressing VMP1 displayed a reduced number of mitochondrial structures, while the number of lysosomal degradation structures was increased. The overexpression of VMP1 did not affect cell proliferation and differentiation, but increased autophagic-flux and improved mitochondrial quality, which coincided with an increased threshold for venetoclax-induced loss of mitochondrial outer membrane permeabilization (MOMP) and apoptosis. In conclusion, our data indicate that in leukemic cells high VMP1 is involved with mitochondrial quality control.

Introduction

Macroautophagy (referred to as autophagy) is a multi-step catabolic process involved in lysosomal degradation of redundant cellular constituents, such as organelles and proteins^{1–3}. Autophagy is essential for hematopoietic stem cell (HSC) maintenance, in part by actively limiting mitochondrial oxidative metabolism^{4,5}. During HSC differentiation the autophagic-flux gradually declines, but autophagy might have distinct functions in terminal differentiated cells⁶. It controls the clearance of

mitochondria in erythroid precursor cells and is essential for monocyte-to-macrophage differentiation^{7–10}. For the malignant counterpart, studies have shown that a subgroup of AML cells heavily relies on autophagy for their survival^{11–13}, whereby increased autophagy is associated with therapy resistance^{14–18}. The increased autophagy is observed especially in poor-risk AML¹¹. Since mutations in autophagy genes have only been observed in the minority of patients¹⁹, increased autophagy is most likely related to other phenomena, such as therapy-induced changes in their metabolism. Inhibition of autophagy by knockdown of essential autophagy genes such as ATG5 or ATG7 impairs AML *in vitro* cell proliferation and *in vivo* engraftment^{11,16,20}. This vulnerability relies on accumulation of (dysfunctional) mitochondria, as evident by the

Correspondence: Edo Vellenga (e.vellenga@umcg.nl)

¹Department of Hematology, Cancer Research Center Groningen, University Medical Center Groningen, University of Groningen, Groningen, The Netherlands

²Department of Laboratory Medicine, University Medical Center Groningen, Groningen, The Netherlands

Edited by M. Diederich

© The Author(s) 2019



Open Access This article is licensed under a Creative Commons Attribution 4.0 International License, which permits use, sharing, adaptation, distribution and reproduction in any medium or format, as long as you give appropriate credit to the original author(s) and the source, provide a link to the Creative Commons license, and indicate if changes were made. The images or other third party material in this article are included in the article's Creative Commons license, unless indicated otherwise in a credit line to the material. If material is not included in the article's Creative Commons license and your intended use is not permitted by statutory regulation or exceeds the permitted use, you will need to obtain permission directly from the copyright holder. To view a copy of this license, visit <http://creativecommons.org/licenses/by/4.0/>.

increased reactive oxygen species (ROS) production and the activation of p53-mediated apoptosis¹¹.

Vacuole membrane protein (VMP1) is an additional autophagy protein residing in the endoplasmic reticulum (ER) membrane^{21,22}, which can interact with the BH3 domain of Beclin-1, thereby activating autophagy²³. The anti-apoptotic BCL-2 family members can also bind to the BH3 domain of Beclin-1, resulting in the dissociation of VMP1 and subsequent inhibition of the autophagic-flux^{23,24}. Little information is available on VMP1 in hematopoietic cells, but in solid tumors it has been shown that VMP1-dependent autophagy can be activated under stress conditions, such as starvation and hypoxia^{25,26}. We therefore determined whether VMP1 is essential for autophagy in normal and malignant hematopoiesis and whether high VMP1 expression provides survival benefits for leukemic cells.

The results showed that VMP1 is important for survival of normal hematopoietic stem cells and progenitor (HSCP) cells *in vitro* and *in vivo*. Moreover, VMP1 expression was significantly increased in AMLs. Overexpression studies and ultrastructurally analysis revealed that VMP1 is involved in mitochondrial quality control, thereby protecting cells against oxidative stress. We concluded that high VMP1 expression increases autophagic flux and the threshold for venetoclax-mediated loss of MOMP and thereby reducing apoptosis-mediated cell death.

Material and methods

Isolation and culture of human CD34⁺ cells

Umbilical cord blood (UCB) obtained from full-term healthy neonates who were born at the Obstetrics departments of the Martini Hospital and the University Medical Center Groningen (Groningen, the Netherlands) after informed consent. AML blasts derived from peripheral blood cells or bone marrow were obtained from patients in accordance with the Declaration of Helsinki; the protocols were approved by the Medical Ethics Committee of the University Medical Center Groningen (UMCG). Mononuclear cells (MNC) were isolated from UCB, or peripheral blood or bone marrow from AML patients by Ficoll density centrifugation, and CD34⁺ cells were subsequently isolated with the autoMACS pro-separator (Miltenyi Biotec, Amsterdam, the Netherlands). With this method CD34⁺ cells are purified twice in order to yield a high purity (>97%). In addition, for FACS-based experiments the CD34⁺ fraction was selected using CD34⁺ markers. AML patient characteristics are indicated in supplemental Table S1. Monoclonal antibodies CD34, CD123, MPO, CD33, HLA-Dr, CD13, CD14, CD15, CD36 were used for determination of the AML phenotype.

Cell culture

Primary AML, normal bone marrow or CB-derived CD34⁺ cells (with a CD34⁺ purity of >97% after isolation) were cultured in suspension or in T25 flasks pre-coated with MS5 stromal cells in Gartners medium: Alpha-MEM (Lonza, Leusden, the Netherlands) supplemented with 12.5% FCS and 12.5% Horse serum (Sigma-Aldrich, Saint Louis, USA), 1% penicillin/streptomycin (PAA Laboratories, Dartmouth, USA), 1 μ M hydrocortisone (Sigma-Aldrich), 57.2 μ M β -mercaptoethanol, and cytokines: G-CSF, Human TPO agonist; Romiplostim (Amgen, Breda, the Netherlands) and IL-3 (20 ng/mL each). The relative increase in Cyto-ID signal after overnight incubation with 20 μ M hydroxychloroquine (HCQ) was defined as the autophagy flux^{6,11}. The concentration and incubation time of HCQ for measuring autophagic-flux was validated and is based on maximal accumulation of autophagosomes, without affecting cell viability, after overnight incubation with HCQ^{6,11}. The leukemic cell lines HL60, OCIM3, MOLM13 and THP1 were obtained from ATCC and the cell lines were all tested mycoplasma free by PCR. All leukemic cell lines cells were cultured in RPMI 1640, supplemented with 10% FCS and 1% penicillin/streptomycin.

Antibodies and reagents

The following anti-human antibodies were used: mouse anti-SQSTM1/p62 (sc-28359) and rabbit (sc-130656) or mouse (sc-47778) anti-Actin, from Santa Cruz (Santa Cruz, CA, USA), Mouse anti-LC3 (5F10, 0231-100) from Nanotools (Munich, Germany), P62, and anti-BCL-2 (Santa Cruz, CA, USA), anti-TOM20 and anti-VMP1 were obtained from cell signalling (Leiden, the Netherlands), Hydroxychloroquine (HCQ), was obtained from Sigma-Aldrich. Venetoclax/ABT-199 (BCL-2 inhibitor, Selleckchem Munich, Germany), S63845 (MCL-1 inhibitor) was obtained from APEXBio (Boston, MA, USA). The pan caspase inhibitor ZVAD-FMK was obtained from (Enzo Life Sciences, Bruxelles, Belgium).

Mitochondrial copy number assay

Total DNA was isolated from $>1 \times 10^5$ cells using RNeasy mini kit (Qiagen, Venlo, the Netherlands). Obtained total DNA was real-time amplified in iQ SYBR Green Supermix (Bio-Rad) with the CFX connect Thermocycler (Bio-Rad). The nuclear genes GAPDH and B2M or mitochondrial genes 12S and tRNA were amplified. The obtained CT values were corrected for the corresponding calculated primer reaction efficiencies. Based on the corrected CT values, the mtDNA copy number was calculated relative to nuclear DNA copy number²⁷. The primer sequences are listed in the Supplemental Table S2.

Virus production and transduction of CD34⁺ leukemic cells or cell lines

Five lentiviral plasmids with short hairpin RNA (shRNA) targeting VMP1 were obtained from GE Healthcare Dharmacon. The shRNAs were cloned into a pLKO.1-mCherry lentiviral vector using MunI & SacII restriction enzymes (Thermo Scientific). After initial testing, two shRNAs (Clone ID TRCN0000135158 and TRCN0000138386) were selected for this study based on effective knockdown efficiency. A shRNA sequence that does not target human genes (referred to as scrambled) was used as a control. Lentiviral virions were produced by transient transfection of HEK 293 T cells with pCMV and VSV-G packing system using Polyethylenimine (Polysciences Inc. Eppelheim, Germany) or FuGENE (Promega, Leiden, the Netherlands). Retroviral virions containing pBABE-puro-mCherry-EGFP-LC3B were produced as described earlier¹¹. Viral supernatants were collected and filtered through a 0.2- μ m filter and subsequently concentrated using Centrprep Ultracel YM-50 centrifugal filters (Millipore, Amsterdam, The Netherlands). CD34⁺ cells were seeded in Gartners medium supplemented with cytokines (specified previously). Transduction was performed by adding 0.5 mL of ~10 times concentrated viral supernatant to 0.5 mL of medium containing 0.5×10^6 cells in the presence of 4 μ g/mL polybrene (Sigma-Aldrich).

ATP assay

Luminescent ATP Detection Assay Kit (Abcam, Cambridge, UK, ab113849) was used to measure the levels of ATP, according to the manufacturer's protocol.

Gene ontology (GO) analysis in AML

Publicly available data of two large AML expression datasets with 460 (GSE6891²⁸ and 173 (TCGA dataset²⁹, samples, respectively, was analysed using the R2 Genomics Analysis and Visualization Platform (<http://r2.amc.nl>). Gene expression data of all genes was correlated with VMP1 expression. Correlations with a p -value of ≥ 0.01 and/or with a correlation coefficient of $r = \leq 0.25$ were discarded. Next, genes which positively or inversely correlated with VMP1 expression in both AML datasets were compared. In total 551 (26.8% overlap) positively correlating genes and 979 (24.1% overlap) inversely correlating genes were present in both datasets. Gene ontology analysis, using David, was performed on the overlapping positively or inversely correlating genes.

Electron microscopy

The experimental procedure for ultrastructural analysis of hematopoietic cells has been described previously³⁰. In brief, FACS sorted OCIM3 cells transduced with pRRL-blueberry or pRRL-VMP1-blueberry and OCIM3 cells

transduced with shSCR-mCherry or shVMP1-mCherry were pelleted and subsequently fixed in 2% paraformaldehyde and 2% glutaraldehyde in 0.1 M cacodylate buffer for 24 h at 4 °C. After fixation the cells were washed in 0.1 M cacodylate buffer. Cells were stained with Evans blue and subsequently embedded in low melting point agarose, as described previously³¹. Agarose pieces containing the cell pellet were dehydrated, osmicated, and embedded in Epon according to routine procedures. Semi-thin sections (0.5 μ m) stained with toluidine blue were inspected using light microscopy to select for OCIM3 cells. Ultra-thin sections (60–80 nm) were cut and stained with 4% uranyl acetate in water, followed by Reynolds lead citrate. Images were taken with a Zeiss Supra55 in STEM (Oberkochen, Germany) mode with ATLAS software developed by Fibics (Ottawa, Ontario, Canada) and the CM100 (Eindhoven, the Netherlands).

In vivo transplantations into NSG mice

Twelve- to thirteen-week-old female NSG (NOD.Cg-Prkdcscid IL2rgtm1Wjl/SzJ) mice were purchased from the Central Animal Facility breeding facility within the UMCG. Mouse experiments were performed in accordance with national and institutional guidelines and all experiments were approved by the Institutional Animal Care and Use Committee of the University of Groningen (IACUC-RuG). The experiment was performed as described previously⁶.

Statistical analysis

An unpaired two-sided Student's t -test or a Mann Whitney U test was used to calculate statistical differences. A p -value of < 0.05 was considered statistically significant.

All tables, additional material and methods sections and supplemental figure legends are available as supplemental information

Results

VMP1 expression is increased in a subset of CD34⁺ AML cells

We previously performed transcriptome analysis on a publicly available gene expression database of normal HSPCs and AML cells (Bloodspot expression database³²), with a focus on autophagy associated genes. This showed that several core-autophagy genes were differentially expressed in AML compared to normal HSPCs¹¹. Further analysis revealed that putative autophagy protein VMP1 was expressed at significantly higher levels in AMLs compared to normal HSPCs (Fig. 1a). In contrast, the expression of the known VMP1 interaction protein Beclin-1 was not different between AML and normal HSPCs (Fig. 1a). The elevated expression of VMP1 was

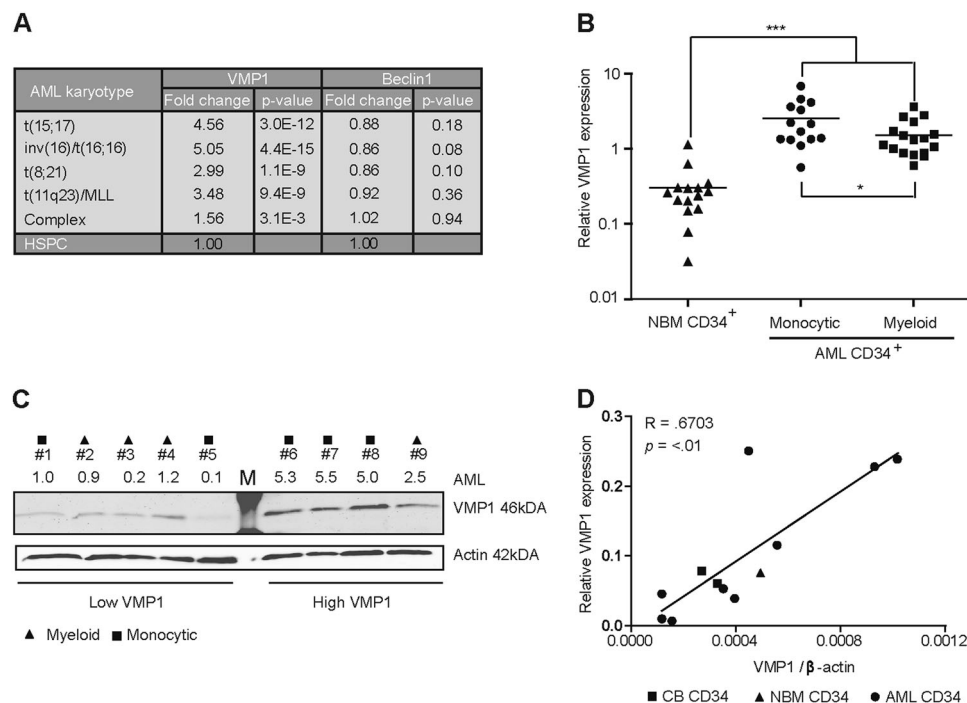


Fig. 1 VMP1 expression is increased in a subset of AMLs. **a** Expression of VMP1 and Beclin-1 in mononuclear primary AML cells acquired from the publicly available expression dataset Bloodspot. HSPC is defined as the combined fractions of HSC, MMP, CMP, GMP and MEP. **b** Gene expression of VMP1 determined by quantitative RT-PCR in normal bone marrow (NBM) CD34⁺ cells ($n = 15$), AMLs with myeloid ($n = 17$) or monocytic characteristics ($n = 14$). **c** Western Blot showing variation in VMP1 protein levels in different AMLs ($n = 9$), β -actin was used as control and VMP1/ β -actin levels are shown relative to AML1. Triangles, squares or circles indicate AMLs with a myeloid or monocytic, respectively. **d** Correlation between VMP1 mRNA levels and protein levels in primary AML CD34⁺ cells ($n = 9$, square symbols), CB CD34⁺ cells ($n = 2$, circles) and NBM CD34⁺ cells ($n = 1$, triangle). Error bars represent SD; * or *** represents $p < .05$ or $p < .001$, respectively

validated by quantitative polymerase chain reaction (qPCR), whereby the highest VMP1 expression was observed in CD34⁺ AMLs with a monocytic phenotype (Fig. 1b). Based on the VMP1 levels in Fig. 1b, AMLs with low or high VMP1 expression were selected for western blot analysis to determine VMP1 protein levels. Western blot analysis confirmed variable protein levels of VMP1 in primary AML CD34⁺ cells ($n = 9$, Fig. 1c). In addition VMP1 mRNA levels significantly correlated ($R = 0.6703$, $p < .01$) with VMP1 protein levels (Fig. 1d, AML ($n = 9$), CB CD34⁺ cells ($n = 2$) and normal bone marrow (NBM) CD34⁺ cells ($n = 1$). Together these findings indicate that VMP1 is overexpressed in a subset of primary AML CD34⁺ cells.

VMP1 knockdown in HSPCs results in inhibition of autophagy and an impaired in vitro expansion and in vivo engraftment

To investigate the functional role of VMP1 in HSPCs and their progeny, human CB-derived CD34⁺ cells were transduced with lentiviral shRNAs targeting VMP1 and subsequently cultured in vitro or transplanted in vivo (Fig. 2a). A panel of five shRNAs was tested, of which two were

selected based on their efficacy. Knockdown of VMP1 in CB CD34⁺ cells was confirmed at the mRNA and protein level with both shVMP1#1 and shVMP1#2 (Fig. 2b). Knockdown of VMP1 resulted in inhibition of the autophagic-flux as determined by relative accumulation of Cyto-ID after HCQ treatment at day 7 during both myeloid and erythroid liquid cultures (Supplemental Fig. S1A). As reported previously⁶, the autophagic-flux was higher under erythroid- compared to myeloid-culture conditions (Supplemental Fig. S1A). A significant reduction in erythroid progenitor (BFU-E) frequency was observed in in vitro colony assays upon knockdown of VMP1 (Fig. 2c), while no change in myeloid colony formation was observed. However, a reduction in relative expansion was observed upon knockdown of VMP1 under both erythroid and myeloid liquid culture conditions (Fig. 2d).

To assess whether VMP1 knockdown would affect the differentiation potential of CB CD34⁺ cells, the expression of myeloid (CD14, CD15) and erythroid differentiation markers (CD71, CD235A) were analysed using flow cytometry. This revealed only a minor delay in CD14 expression at day 8 (Supplemental Fig. S1B), but a

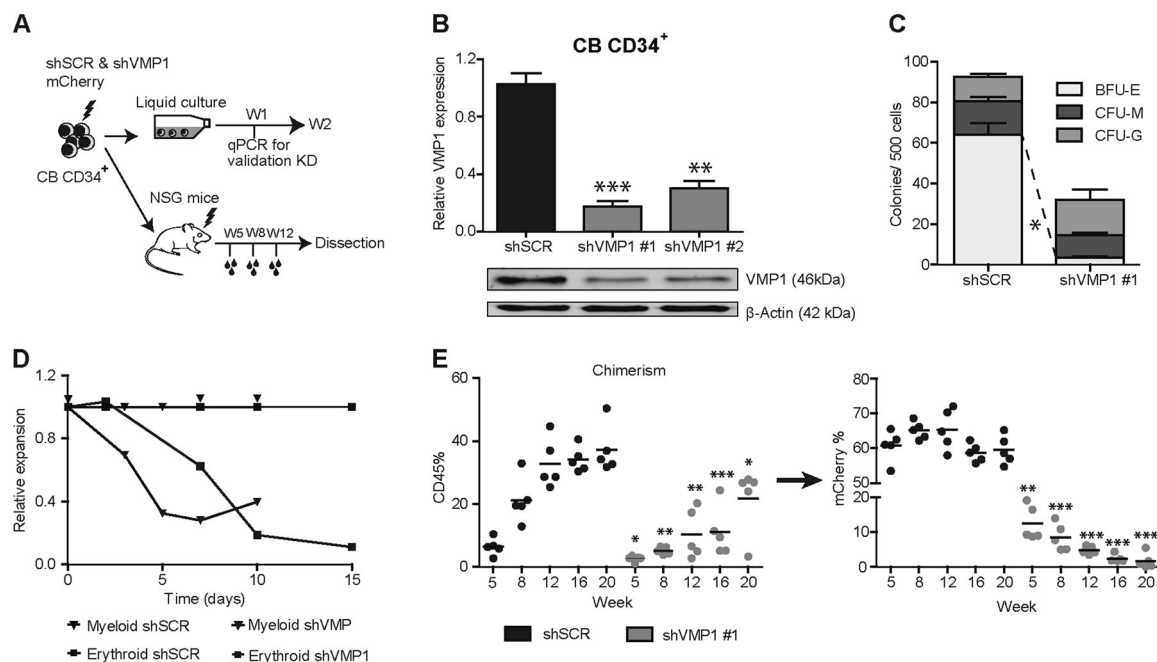


Fig. 2 VMP1 knockdown in HSPCs results in inhibition of autophagy and an impaired in vitro expansion and in vivo engraftment. a

Experimental scheme, shSCR-mCherry or shVMP1-mCherry transduced cord blood (CB) CD34⁺ cells were cultured in vitro under myeloid or erythroid liquid culture conditions or injected IV in sub-lethally irradiated NSG mice. Bleeds were performed at week 5, 8, and 12 after injection and analysed by FACS. **b** Knockdown efficiency of VMP1 was determined by quantitative RT-PCR and Western blotting of CB CD34⁺ cells transduced with shSCR, shVMP1 #1 or shVMP1 #2. **c** CFC assay with freshly sorted shSCR or shVMP1 #1 transduced CB CD34⁺ cells ($n = 2$). **d** Representative graph showing relative expansion of shVMP1 transduced CB CD34⁺ cells under myeloid or erythroid permissive liquid culture conditions, shSCR transduced cells were used as control ($n = 2$). **e** Percentage of engraftment represented by huCD45 percentage (left graph) and the percentage mCherry within the huCD45⁺ population (right graph). Each dot represents data from a single mouse, $n = 5$ for each group. Error bars represent SD; *, ** or *** represents $p < .05$, $p < .01$ or $p < .001$, respectively

stronger effect on terminal erythroid differentiation (Supplemental Fig. S1C). To study the long-term effects of VMP1 knock-down in the context of the micro-environment, transduced CD34⁺ HSPCs were cultured on MS5 bone marrow stromal co-cultures, in which VMP1 knockdown resulted in reduced expansion, as determined by the decline in percentage of mCherry positive cells (Supplemental Fig. S1D). The negative phenotype of shVMP1-transduced HSPCs was at least in part caused by increased apoptosis (Supplemental Fig. S1E), while cell cycle progression was not affected (Supplemental Fig. S1F). To assess whether VMP1 knockdown also affected in vivo engraftment, unsorted shSCR or shVMP1-mCherry-transduced CB CD34⁺ cells were transplanted into immunodeficient NSG mice (Fig. 2a). Transplanted CD34⁺ cells were ~60% mCherry-positive. Engraftment, as determined by the percentage huCD45 in peripheral blood, was significantly reduced in shVMP1 mice compared to controls (Fig. 2e, left panel). While mCherry levels for shSCR remained stable around ~60%, the contribution of the shVMP1 transduced cells to the engrafted cells over time was significantly reduced in mice with transplanted shVMP1 CD34⁺ cells, compared to controls

(Fig. 2e, right panels). At sacrifice, high engraftment levels in bone marrow, spleen and liver were observed, and the contribution of shSCR-mCherry transduced cells within the CD45 compartment was around ~60% in all analyzed organs (Supplemental Fig. S1G, left panel). In contrast, the percentage of shVMP1-mCherry transduced cells within the CD45 compartment was strongly reduced (Supplemental Fig. 1G, right panel). Together these findings indicate that knockdown of VMP1 inhibits autophagic-flux and results in reduced expansion of HSPC, delayed differentiation and an impaired long-term engraftment in vivo.

VMP1 knockdown results in inhibition of autophagy, impaired expansion, increased apoptosis and reduced cell cycle progression in leukemic cells

Because VMP1 was shown to be differentially expressed in primary leukemic CD34⁺ cells and leukemic cell lines (Fig. 1, Supplementary Fig. 2A), the consequences of VMP1 modulation were assessed in leukemic cells. First, leukemic cell lines with previously determined autophagy activity¹¹ were transduced with shVMP1 or shSCR lentivectors and knockdown efficiencies were confirmed at the

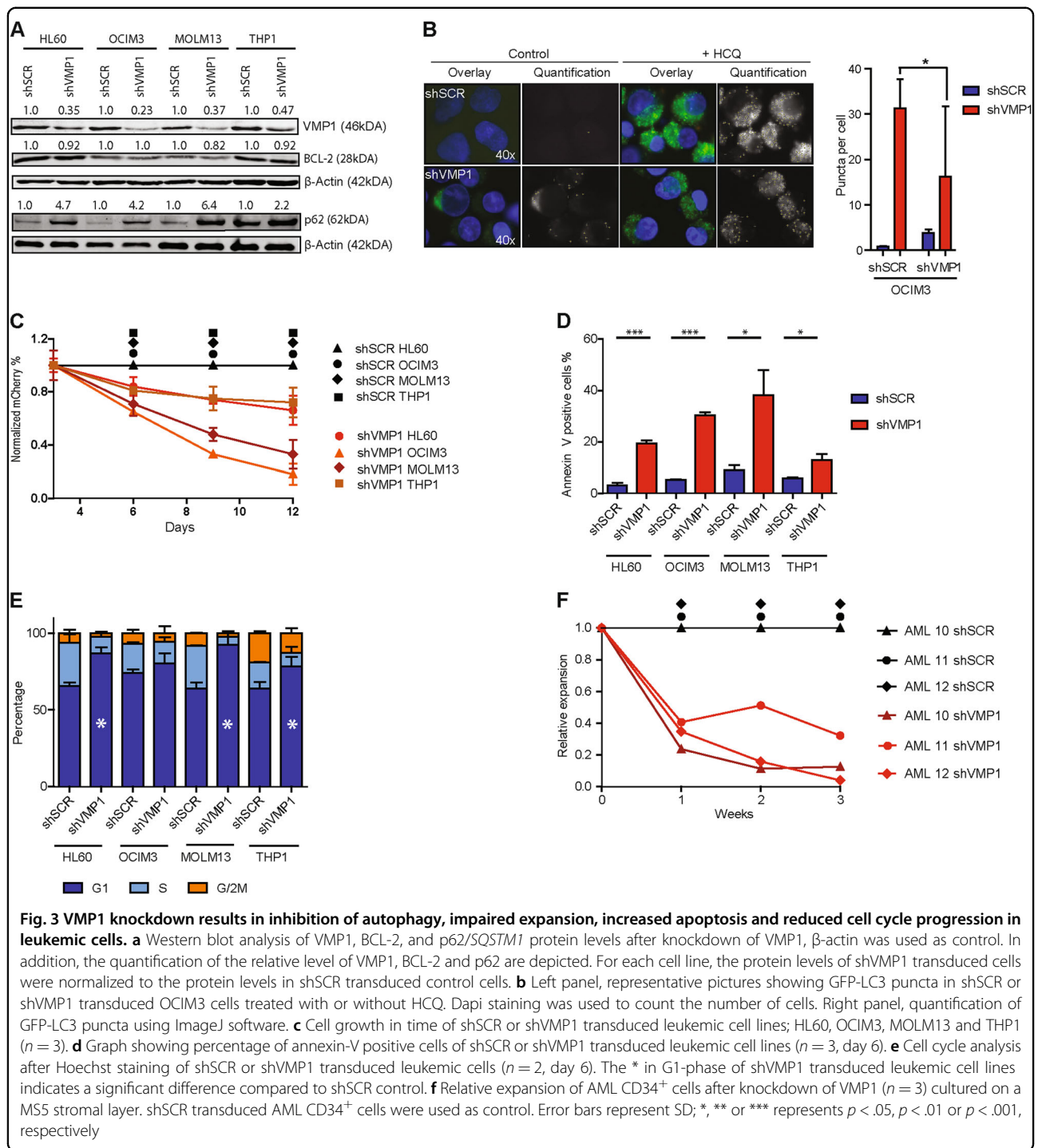
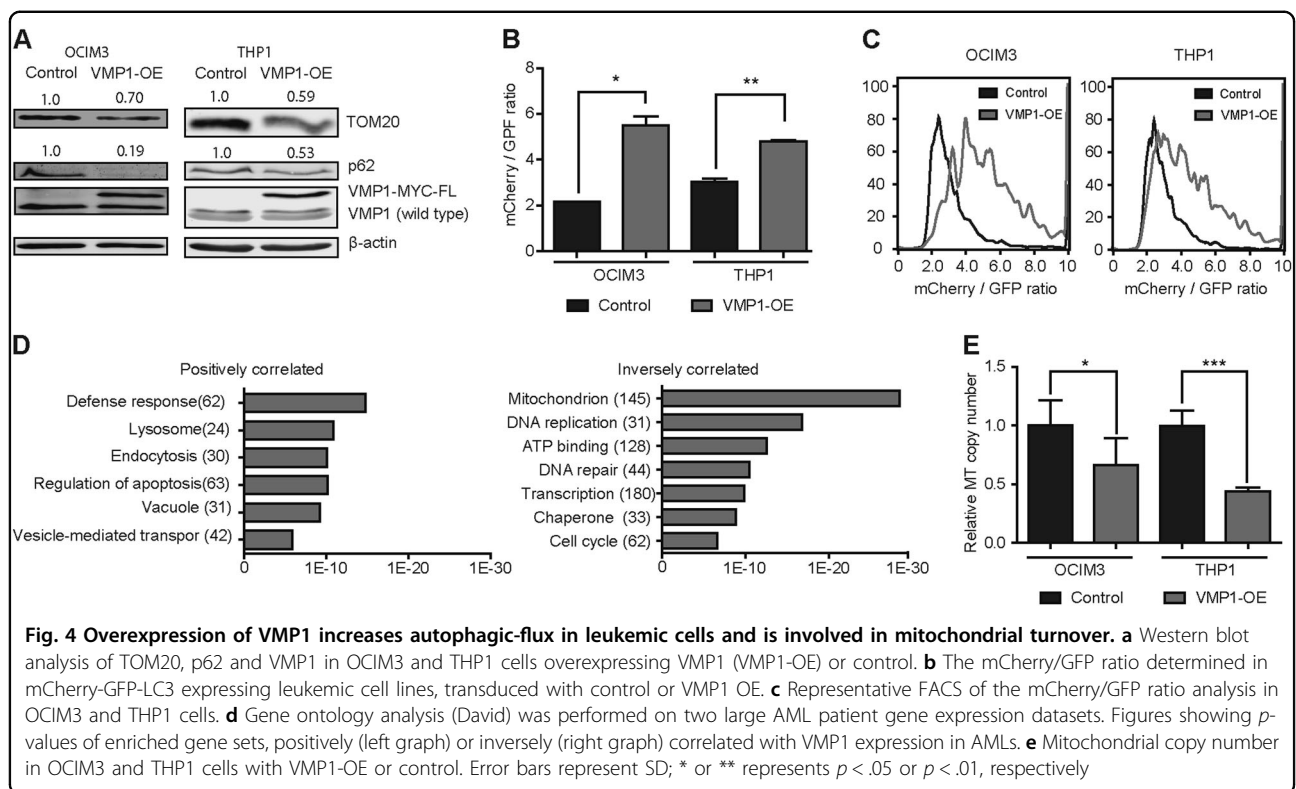


Fig. 3 VMP1 knockdown results in inhibition of autophagy, impaired expansion, increased apoptosis and reduced cell cycle progression in leukemic cells. **a** Western blot analysis of VMP1, BCL-2, and p62/SQSTM1 protein levels after knockdown of VMP1, β-actin was used as control. In addition, the quantification of the relative level of VMP1, BCL-2 and p62 are depicted. For each cell line, the protein levels of shVMP1 transduced cells were normalized to the protein levels in shSCR transduced control cells. **b** Left panel, representative pictures showing GFP-LC3 puncta in shSCR or shVMP1 transduced OCIM3 cells treated with or without HCQ. Dapi staining was used to count the number of cells. Right panel, quantification of GFP-LC3 puncta using ImageJ software. **c** Cell growth in time of shSCR or shVMP1 transduced leukemic cell lines; HL60, OCIM3, MOLM13 and THP1 ($n = 3$). **d** Graph showing percentage of annexin-V positive cells of shSCR or shVMP1 transduced leukemic cell lines ($n = 3$, day 6). **e** Cell cycle analysis after Hoechst staining of shSCR or shVMP1 transduced leukemic cells ($n = 2$, day 6). The * in G1-phase of shVMP1 transduced leukemic cell lines indicates a significant difference compared to shSCR control. **f** Relative expansion of AML CD34⁺ cells after knockdown of VMP1 ($n = 3$) cultured on a MS5 stromal layer. shSCR transduced AML CD34⁺ cells were used as control. Error bars represent SD; *, ** or *** represents $p < .05$, $p < .01$ or $p < .001$, respectively

protein level, while BCL-2 levels were not affected (Fig. 3a). Knockdown of VMP1 was associated with impaired autophagy, reflected by accumulation of SQSTM1/p62 (Fig. 3a) and reduced accumulation of LC3 puncta after HCQ treatment³³ (Fig. 3b, Supplemental Fig. S2B). The knockdown of VMP1 had a strong impact on cell growth (Fig. 3c), which was at least in part due to increased

apoptosis, as determined by annexin-V positivity (Fig. 3d). The addition of the pan caspase inhibitor ZVAD-FMK partially rescued the observed phenotype (Supplemental Fig. S2C). In addition, cell cycle analysis showed that cells accumulated in G1 phase significantly (Fig. 3e). Next, AML patient-derived CD34⁺ ($n = 3$) cells were transduced with shVMP1-mCherry or shSCR-mCherry. The



unsorted cells were cultured long-term in MS5 bone marrow stromal cocultures. The transduction efficiency in AML CD34⁺ cells was between 20–60% and comparable between shSCR and shVMP1 within a single AML sample (Supplemental Fig. S2D). After 4 days of culture the knockdown of VMP1 was 33 and 48% in AML10 and AML12 respectively. Similar to leukemic cell lines, knockdown of VMP1 resulted in decreased expansion of primary AML CD34⁺ cells, relative to scrambled control (Fig. 3f). Together, these results indicate that VMP1 is essential for survival and proliferation of leukemic cell lines and patient-derived AML CD34⁺ cells.

Overexpression of VMP1 increases autophagic-flux in leukemic cells and is involved in mitochondrial turnover

To study the consequences of high expression of VMP1 on normal and leukemic hematopoietic cells, a lentiviral VMP1-Blueberry overexpression vector (VMP1-OE) was constructed, and overexpression of VMP1 was confirmed at the protein level (Fig. 4a). Overexpression resulted in reduced p62/SQSTM1 protein levels. (Fig. 4a). Decreased p62/SQSTM1 accumulation was confirmed by blocking autophagy at a late stage using HCQ (Supplemental Fig. S3A). In addition, overexpression of VMP1 resulted in increased relative Cyto-ID MFI, which reflects a higher LC3-dependent autophagy activity (Supplemental Fig. S3B). Next, leukemic cell lines expressing the mCherry-GFP-LC3 autophagy reporter were transduced with

control or VMP1-OE cells to assess the impact on the autophagy flux. An increased mCherry/GFP ratio was observed in OCIM3 and THP1 cells overexpressing VMP1, confirming that the LC3-dependent autophagy-flux was increased (Fig. 4b–c). The increased autophagy did not affect the cell proliferation of the cell lines.

To obtain more insight into the role of VMP1 in AML, two large AML expression datasets^{28,29} were analysed using the R2 Genomics Analysis and Visualization Platform. Gene ontology analyses (GO) was performed on genes correlating with VMP1 expression. GO analysis revealed that positively correlated genes were enriched for the GO terms lysosome, vacuole and vesicle transport, while inversely correlated genes were enriched for the GO terms mitochondrion, DNA replication, ATP binding, apoptosis and cell cycle (Fig. 4d). Because high VMP1 expression in AML cells is inversely correlated with gene signatures associated with mitochondria (Fig. 4d, right panel), mitochondrial function was assessed after modulation of VMP1 expression. Overexpression of VMP1 led to a significant decrease in mitochondrial DNA (mtDNA) copy number relative to nuclear DNA (nucDNA) in OCIM3 and THP1 cells (Fig. 4e). In line with these results, TOM20 which is a marker for mitochondrial mass, was decreased after overexpression of VMP1 (Fig. 4a). Conversely, shVMP1 transduced leukemic cells had an increase in mtDNA copy number in cell lines. (Supplemental Fig. S3C). However, this increase was not

observed in MOLM13 cells. Together these findings indicate that overexpression of VMP1 is involved in mitochondrial turnover.

Ultrastructural analysis and mitochondrial function in OCIM3 cells after VMP1 modulation

To obtain more insight into the involvement of VMP1 in mitochondrial quality control, we analyzed OCIM3 cells ultrastructurally with electron microscopy (EM) after lentiviral overexpression or knockdown of VMP1. OCIM3 cells overexpressing VMP1 displayed a reduction in the number of mitochondrial structures compared to control cells (Fig. 5a, $p < .01$). Representative ultrastructural images are shown in Fig. 5b. In the shVMP1-transduced OCIM3 cells mitochondria were on average ~24% larger and swollen compared to control (Supplemental Fig. 4A). Moreover, in contrast to VMP1-OE, cells with knockdown of VMP1 had elevated numbers of mitochondrial structures (Fig. 5c–d, $p < .05$). In addition, the mitochondrial function was analyzed after VMP1 modulation. The mitochondrial membrane potential (MMP) measured by tetramethylrhodamine (TMRM) was significantly increased in OCIM3 cells overexpressing VMP1, while there was a trend for reduced MMP upon VMP1 knockdown (Fig. 5e). Although the number of mitochondria in VMP1 overexpressing cells was reduced (Fig. 4), these cells had higher levels of ATP content (Fig. 5f). Conversely, knockdown of VMP1 resulted in decreased ATP production with concomitant increased ROS levels, indicating a loss in mitochondrial function (Fig. 5f, Supplemental Fig. S4B–C). In line with these results, increased ROS levels were also observed with the Mito-SOX tracer confirming that ROS is of mitochondria origin (Supplemental Fig. S4, D). Additional analysis by EM revealed that cells overexpressing VMP1 had an increased number of onion-like multilamellar membrane structures, also called whorls (Fig. 5a, g, 1.5 fold, $p < .05$). These structures are associated with lysosomal mediated degradation of intra-cellular parts, also termed the degradative compartment³⁴, and are associated with an increased autophagy flux. Together, the increase in autophagy, the reduced number of mitochondria structures in response to VMP1 overexpression are indicative of increased turnover of mitochondria.

Overexpression of VMP1 interferes with venetoclax induced apoptosis

BCL-2 protein family members regulate apoptosis by controlling the permeability of mitochondria³⁵. Interestingly, VMP1 has been shown to contain a BH3-binding domain, which is an important characteristic of the BCL-2 protein family³⁶. The specific BCL-2 inhibitor venetoclax has been shown to disrupt the BH3 dependent BCL-2/Beclin-1 interaction, thereby activating autophagy^{37,38}.

First, we studied the consequences for autophagy activity after venetoclax treatment in the context of high VMP1 expression. As expected, in THP1 cells p62 levels declined in a dose-dependent manner with increasing concentration of venetoclax, which is indicative for increased autophagic-flux (Fig. 6a). Basal p62 levels were reduced in THP1 cells overexpressing VMP1, while p62 levels further declined with increasing concentrations of venetoclax (Fig. 6a). Next, we evaluated the effect of high VMP1 expression on the threshold for mitochondrial outer membrane permeabilization (MOMP). The initiation of MOMP is preceded by loss of mitochondrial membrane potential (MMP) and results in caspase-dependent apoptosis³⁵. Leukemic cells overexpressing either BCL-2 or VMP1 were treated with increasing concentrations of venetoclax and the MMP was determined after tetramethylrhodamine (TMRM) staining in the context of BCL-2 and VMP1 overexpression. Venetoclax-induced loss of MMP could be partially rescued by VMP1 or BCL-2 overexpression (Fig. 6b and Supplemental Fig. 5A). In addition, venetoclax induced apoptotic response in HL60 and THP1 cells, as determined by caspase-3 cleavage and annexin-V staining, could partially be rescued by overexpressing BCL-2 or VMP1 (Fig. 6c–d and Supplemental Fig. S5A). Inhibition of autophagy with HCQ did not reverse the VMP1-mediated rescue of venetoclax cytotoxicity (Supplementary Fig. 5B). Next, we validated whether inhibition of autophagy by knocking down VMP1 or the essential autophagy gene ATG7 would affect venetoclax mediated cell death. In contrast to overexpression of VMP1, knockdown of VMP1 or ATG7 in combination with venetoclax treatment resulted in enhanced cell death, although no synergistic effects were observed with the combination (shVMP1 $31 \pm 3.7\%$ vs. shVMP1 plus venetoclax $53 \pm 3.7\%$ reduction in survival $p < 0.05$ and shATG7 $18\% \pm 2.8\%$ vs. shATG7 plus venetoclax $45 \pm 2.5\%$ reduction in survival $p < 0.01$).

To study the specificity of effects, leukemic cell lines were treated with the specific and potent MCL-1 inhibitor S63845³⁹. In contrast to BCL-2 overexpression, VMP1 overexpression did not rescue S63845-mediated apoptosis (Supplemental Fig. S5C). Finally we tested if high VMP1 expression would affect BCL-2 expression or cellular localization. BCL-2 protein levels did not change after treatment with increasing concentrations of venetoclax in VMP1 overexpressing cells (Supplemental Fig. S5D). Next, cellular fractionation was performed of HL60 cells overexpressing VMP1 or control vector. From total cell lysates the mitochondrial (P10), cytosolic S100 or endoplasmic reticulum fraction (P100) were purified. Purification of the mitochondrial fraction and cytosolic fraction was confirmed by enrichment for COX-IV or β -actin, respectively. Interestingly, under all tested conditions BCL-2 was primarily present in the mitochondrial

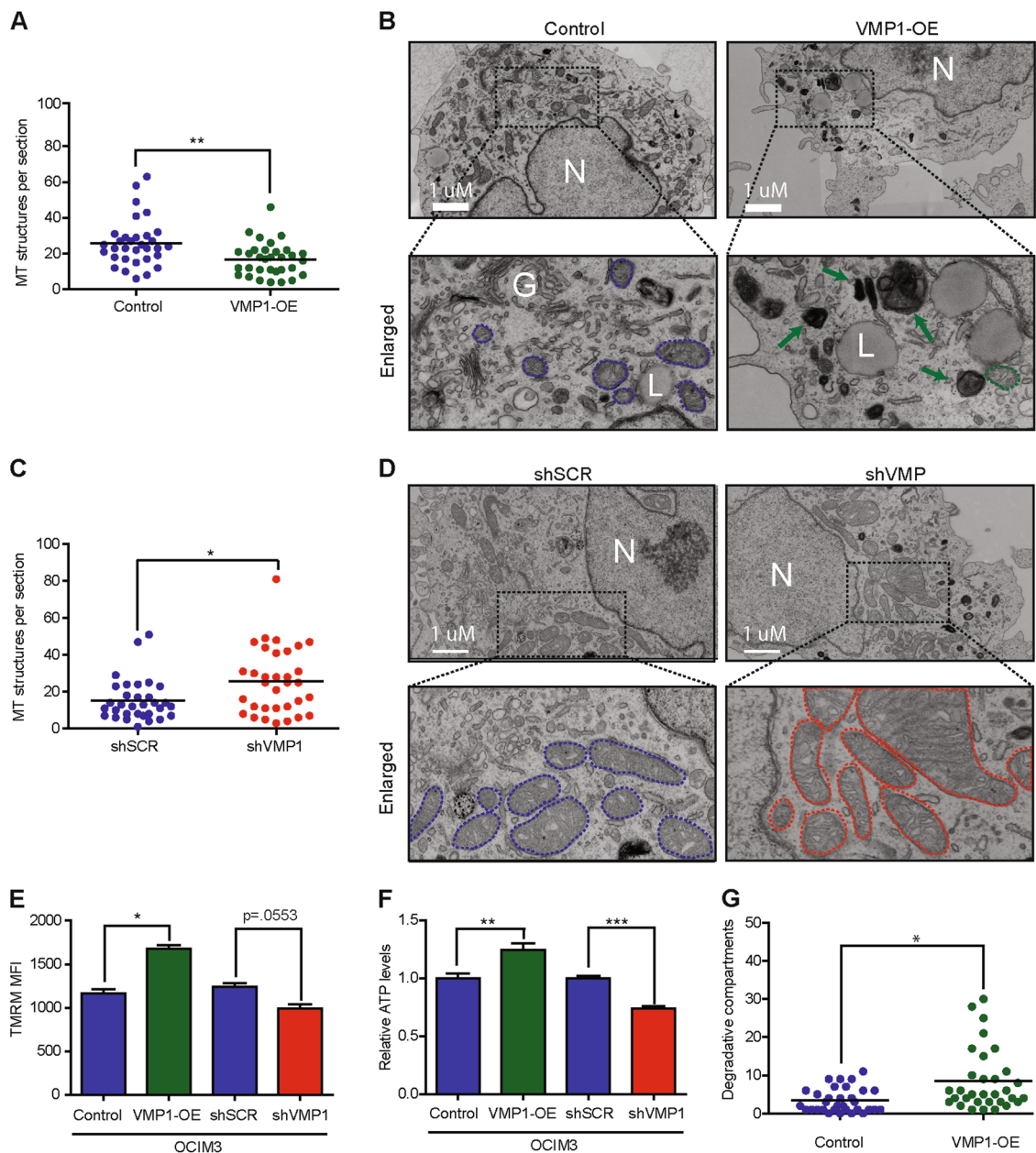


Fig. 5 Ultrastructural analysis and mitochondrial function in OCIM3 cells after VMP1 modulation. **a** Quantification of mitochondrial structures per section in OCIM3 cells transduced with lentiviral vectors for overexpression of VMP1 (VMP1-OE) or control ($n > 32$ sections per group). **b** Representative ultrastructural pictures of OCIM3 cells overexpression VMP1 or control, N = nucleus, L = lipid droplet, G = Golgi, green arrow = whorls/degradative compartments. The blue (control) or green (VMP1-OE) dotted lines indicate mitochondrial structures. **c** Quantification of mitochondrial structures per section in OCIM3 cells with knockdown of VMP1 (shVMP1) or control vectors ($n > 32$ sections per group). **d** Representative ultrastructural pictures of OCIM3 cells with knockdown of VMP1 or control. N = nucleus. The blue (control) or red (shVMP1) dotted lines indicate mitochondrial structures. **e** FACS analysis of mitochondrial membrane potential (MMP) after tetramethylrhodamine (TMRM) staining in OCIM3 with VMP1 overexpression, VMP1 knockdown or control ($n = 3$). **f** ATP levels measured in OCIM3 with VMP1 overexpression, VMP1 knockdown or control ($n = 4$). **g** Electron microscopy, quantification of onion-like multilamellar membrane structures called degradative compartments per section of OCIM3 cells, transduced with VMP1-OE or control ($n \leq 35$ cells per group). Examples of degradative compartments are indicated by green arrows in **b** right panels. Error bars represent SD; * or ** represents $p < .05$ or $p < .01$, respectively

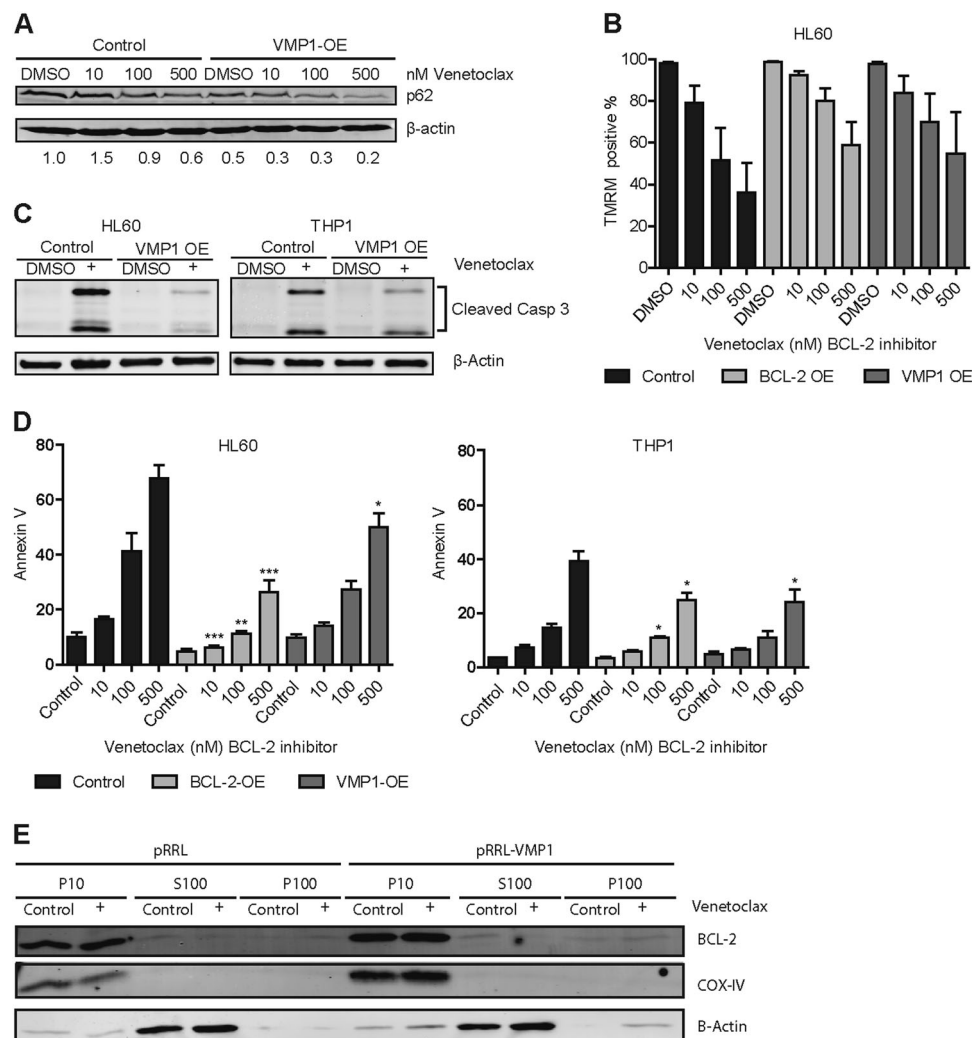


Fig. 6 Overexpression of VMP1 interferes with venetoclax induced apoptosis. **a** Western blot of p62 in THP1 cells overexpressing VMP1 or control treated with different concentrations of venetoclax, β -actin was used as control. ($n = 2$) **b** Bar graph showing the percentage of TMRM positive cells. HL60 cells overexpressing VMP1, BCL-2 or control were incubated for 24 h with different concentrations of venetoclax. ($n = 3$) **c** Western Blot showing cleaved caspase 3 in HL60 and THP1 cells overexpressing VMP1 or control after 24 h incubation with 25 nM venetoclax ($n = 2$). **d** Leukemic cell lines with lentiviral overexpression of VMP1, BCL-2 or control were treated 24 h with venetoclax and apoptosis was measured by annexin-V staining with FACS ($n = 4$). **e** Western blot showing BCL-2, COX-IV, and β -Actin in the mitochondrial (P10), cytosolic (S100) or endoplasmic reticulum (P100) fractions of HL60 cells overexpressing VMP1 or control, treated with or without venetoclax. Error bars represent SD; *, ** or *** represents $p < .05$, $p < .01$ or $p < .001$, respectively

fraction, suggesting that relocalization of BCL-2 did not cause the observed resistance against venetoclax-mediated cell death in high VMP1 expressing cells (Fig. 6e).

Together, these data indicate that overexpression of BCL-2 and VMP1 increase the threshold for venetoclax-mediated loss of MOMP, thereby reducing apoptosis-mediated cell death.

Discussion

The present study indicates that VMP1 is involved in autophagy and mitochondrial turn-over in normal

hematopoietic and leukemic cells. Blocking VMP1 expression impairs the autophagy flux, coinciding with reduced proliferation and survival of normal and leukemic HSPC and impaired in vivo engraftment. Previous studies on VMP1 function have been done primarily in solid tumors^{40,41}, but gene expression studies in hematopoietic cells showed that VMP1 is differentially expressed in hematopoietic cell lineages, including HSPCs. In the leukemic counterpart, VMP1 can be overexpressed in all AML subcategories independent of the molecular and genetic makeup. Functional studies have shown that VMP1 disrupts the binding of BCL-2 to Beclin-1 and

consequently de-represses autophagy²³. These findings are in line with our results showing that reduced VMP1 expression resulted in inhibition of LC3-dependent autophagy, while overexpression enhanced LC3-dependent autophagy-flux. This would also suggest that AMLs with high VMP1 expression are primed for robust autophagy activation in response to cellular stress. In addition, our study showed that high VMP1 expression is inversely correlated with genes enriched for the GO-terms associated with mitochondria, which is in line with studies in Hela cells showing that VMP1 co-localizes with mitochondrial structures^{34,37}. Based on functional studies and electron microscopy, our results suggest that VMP1 regulates mitochondrial quantity and quality by affecting mitophagy. Higher VMP1 expression reduces mitochondrial copy number and TOM20 expression and increases mitochondrial membrane potential and ATP production. This is indicative for improvement in quality of the remaining mitochondria, while reduced VMP1 expression generated the opposite results. In addition, knockdown of VMP1 resulted in swollen mitochondria and increased ROS levels, which is most likely the consequence of accumulating (dysfunction) mitochondria, resulting in cell death which coincides with the loss of mitochondrial membrane potential and ATP levels. Previous studies with ATG12, ATG5 or ATG7 knockout mice have reported comparable results: accumulating dysfunctional mitochondria and ROS^{5,42–44}.

The higher expression of VMP1 in AML CD34⁺ cells might be protective for AML cells in the hypoxic bone marrow micro-environment, where control of mitochondria content and ROS production by autophagy is crucial for maintaining an immature phenotype⁵. Similar to other pro-autophagy genes⁴⁵, VMP1 expression can be upregulated under hypoxia⁴⁶. However, in leukemic cell lines TOM20 and VMP1 protein levels both declined when the cells were cultured under hypoxia (data not shown). Therefore it is more likely that the mitochondrial turnover during hypoxia is controlled by BNIP3 and BNIP3-L, which demonstrate a strong upregulation in response to hypoxia exposure⁴⁵.

The threshold for MOMP, and consequently for cytochrome-c release-dependent caspase activation, is regulated by the expression level of BCL-2 protein family members, which might account for drug resistance in a subgroup of AML patients^{47–50}. Recently, promising results have been obtained with venetoclax in relapsing AML patients in conjunction with low-dose chemotherapy⁵¹. Predictive markers have been identified for reduced sensitivity for venetoclax, such as increased expression of BCL-XL or MCL-1^{39,47,52,53}. The present study indicates that VMP1 overexpression is an additional predictive maker for resistance against venetoclax in AML. VMP1 overexpression resulted in an increase in MMP, which

could in turn increase the threshold for venetoclax-mediated apoptosis. Mitochondria play a central role in regulation of apoptosis⁵⁴. Cells with more mitochondrial content were shown to be more prone to undergo apoptosis⁵⁵. Therefore, VMP1 overexpression could potentially inhibit pro-apoptotic signalling by increased turnover of dysfunctional mitochondria. However, these protective effects of VMP1 are only partially regulated by autophagy induction since HCQ did not reverse the VMP1-mediated rescue of venetoclax induced apoptosis.

In summary, the results demonstrate that VMP1 is essential for HSPC and AML cells and is involved in mitochondrial quality control. High VMP1 expression is protective against loss of membrane potential and apoptosis induced by venetoclax.

Acknowledgements

We kindly thank Prof. Robert E. Campbell (Department of Chemistry, University of Alberta, Edmonton, Alberta, Canada) for providing the mBlueberry Fluorescent Protein. In addition, we would like to thank Dr. Tom van Meerten for providing venetoclax and Mylène Gerritsen for help with cloning the BCL-2-OE and VMP1-OE vectors. We would like to thank Anouk H.G. Wolters for technical assistance with the sample preparations for electron microscopy analysis. Finally, we would like to thank Eva van den Berg and André B. Mulder for cytogenetic and mutation analysis of AML patient samples. Part of the work was performed at the UMCG Microscopy and Imaging Center (UMIC) using the Zeiss Supra55 ATLAS, funded by ZonMW grant 91111.006. This research project was supported by a grant of the Dutch Cancer Foundation (KWF, 2010-4771). The GFP-mCherry-LC3 vector was a kind gift of Prof. Andrew Thorburn, Dept. of Pharmacology, University of Colorado Cancer Center).

Authors contributions

H.F.: conception and design, collection and/or assembly of data, data analysis and interpretation, and manuscript writing. A.T.W. and F.A.v.d.H.: data analysis and interpretation; J.J.S. and E.V.: conception and design, data analysis and interpretation, financial support, administrative support, final approval of manuscript; H.F., A.T.W., J.J.S. and E.V. conceived and designed the experiments; H.F., F.A.v.d.H., R.R.W., D.S.K. and J.J. performed the experiments; H.F., A.T.W., J.J.S. and E.V. analyzed the data; H.F., J.J.S. and E.V. wrote the paper.

Conflict of interest

The authors declare that they have no conflict of interest.

Publisher's note

Springer Nature remains neutral with regard to jurisdictional claims in published maps and institutional affiliations.

Supplementary Information accompanies this paper at (<https://doi.org/10.1038/s41419-019-1648-4>).

Received: 19 November 2018 Revised: 9 May 2019 Accepted: 13 May 2019
Published online: 29 May 2019

References

- Luo, C. et al. Mitochondrial accumulation under oxidative stress is due to defects in autophagy. *J. Cell Biochem.* **114**, 212–219 (2013).
- Joshi, A. & Kundu, M. Mitophagy in hematopoietic stem cells: the case for exploration. *Autophagy* **9**, 1737–1749 (2013).
- Yang, Z. & Klionsky, D. J. Eaten alive: a history of macroautophagy. *Nat. Cell Biol.* **12**, 814–822 (2010).
- Leveque-El Moutte, L. et al. Autophagy is required for stem cell mobilization by G-CSF. *Blood* **125**, 2933–2936 (2015).

5. Ho, T. T. et al. Autophagy maintains the metabolism and function of young and old stem cells. *Nature* **543**, 205–210 (2017).
6. Gomez-Puerto, M. C. et al. Autophagy proteins ATG5 and ATG7 are essential for the maintenance of human CD34(+) hematopoietic stem-progenitor cells. *Stem Cells* **34**, 1651–1663 (2016).
7. Zhang, Y., Morgan, M. J., Chen, K., Choksi, S. & Liu, Z. G. Induction of autophagy is essential for monocyte-macrophage differentiation. *Blood* **119**, 2895–2905 (2012).
8. Kundu, M. et al. Ulk1 plays a critical role in the autophagic clearance of mitochondria and ribosomes during reticulocyte maturation. *Blood* **112**, 1493–1502 (2008).
9. Betin, V. M., Singleton, B. K., Parsons, S. F., Anstee, D. J. & Lane, J. D. Autophagy facilitates organelle clearance during differentiation of human erythroblasts: evidence for a role for ATG4 paralogs during autophagosome maturation. *Autophagy* **9**, 881–893 (2013).
10. Zhang, J. et al. Mitochondrial clearance is regulated by Atg7-dependent and -independent mechanisms during reticulocyte maturation. *Blood* **114**, 157–164 (2009).
11. Folkerts, H. et al. Inhibition of autophagy as a treatment strategy for p53 wild-type acute myeloid leukemia. *Cell Death Dis.* **8**, e2927 (2017).
12. Man, N. et al. Caspase-3 controls AML1-ETO-driven leukemogenesis via autophagy modulation in a ULK1-dependent manner. *Blood* **129**, 2782–2792 (2017).
13. Rudat, S. et al. RET-mediated autophagy suppression as targetable co-dependence in acute myeloid leukemia. *Leukemia* **32**, 2189–2202 (2018).
14. Auberger, P. & Puissant, A. Autophagy, a key mechanism of oncogenesis and resistance in leukemia. *Blood* **129**, 547–552 (2017).
15. Piya, S. et al. Atg7 suppression enhances chemotherapeutic agent sensitivity and overcomes stroma-mediated chemoresistance in acute myeloid leukemia. *Blood* **128**, 1260–1269 (2016).
16. Sumitomo, Y. et al. Cytoprotective autophagy maintains leukemia-initiating cells in murine myeloid leukemia. *Blood* **128**, 1614–1624 (2016).
17. Stankov, M. V. et al. Histone deacetylase inhibitors induce apoptosis in myeloid leukemia by suppressing autophagy. *Leukemia* **28**, 577–588 (2014).
18. Altman, J. K. et al. Autophagy is a survival mechanism of acute myelogenous leukemia precursors during dual mTORC2/mTORC1 targeting. *Clin. Cancer Res.* **20**, 2400–2409 (2014).
19. Visconte, V. et al. Complete mutational spectrum of the autophagy inter-actome: a novel class of tumor suppressor genes in myeloid neoplasms. *Leukemia* **31**, 505–510 (2017).
20. Liu, Q., Chen, L., Atkinson, J. M., Claxton, D. F. & Wang, H. G. Atg5-dependent autophagy contributes to the development of acute myeloid leukemia in an MLL-AF9-driven mouse model. *Cell Death Dis.* **7**, e2361 (2016).
21. Zhao, Y. G. et al. The ER-localized transmembrane protein EPG3/VMP1 regulates SERCA activity to control ER-isolation membrane contacts for autophagosome formation. *Mol. Cell* **67**, 974–989 (2017).
22. Nascimbeni, A. C. et al. ER-plasma membrane contact sites contribute to autophagosome biogenesis by regulation of local PI3P synthesis. *EMBO J* **36**, 2018–2033 (2017).
23. Molejon, M. I., Ropolo, A. & Vaccaro, M. I. VMP1 is a new player in the regulation of the autophagy-specific phosphatidylinositol 3-kinase complex activation. *Autophagy* **9**, 933–935 (2013).
24. Erlich, S. et al. Differential interactions between Beclin 1 and Bcl-2 family members. *Autophagy* **3**, 561–568 (2007).
25. Guo, L., Yang, L. Y., Fan, C., Chen, G. D. & Wu, F. Novel roles of Vmp1: inhibition metastasis and proliferation of hepatocellular carcinoma. *Cancer Sci* **103**, 2110–2119 (2012).
26. Ropolo, A. et al. The pancreatitis-induced vacuole membrane protein 1 triggers autophagy in mammalian cells. *J. Biol. Chem.* **282**, 37124–37133 (2007).
27. Rooney, J. P. et al. PCR based determination of mitochondrial DNA copy number in multiple species. *Methods Mol. Biol.* **1241**, 23–38 (2015).
28. de Jonge, H. J. et al. High VEGFC expression is associated with unique gene expression profiles and predicts adverse prognosis in pediatric and adult acute myeloid leukemia. *Blood* **116**, 1747–1754 (2010).
29. Ley, T. J. et al. Genomic and epigenomic landscapes of adult de novo acute myeloid leukemia. *N. Engl. J. Med.* **368**, 2059–2074 (2013).
30. Houwerzijl, E. J. et al. Increased peripheral platelet destruction and caspase-3-independent programmed cell death of bone marrow megakaryocytes in myelodysplastic patients. *Blood* **105**, 3472–3479 (2005).
31. Carper, D., Smith-Gill, S. J. & Kinoshita, J. H. Immunocytochemical localization of the 27K beta-crystallin polypeptide in the mouse lens during development using a specific monoclonal antibody: implications for cataract formation in the Philly mouse. *Dev. Biol.* **113**, 104–109 (1986).
32. Bagger, F. O. et al. BloodSpot: a database of gene expression profiles and transcriptional programs for healthy and malignant haematopoiesis. *Nucleic Acids Res.* **44**(D1), 917–924 (2016).
33. Klionsky, D. J. et al. Guidelines for the use and interpretation of assays for monitoring autophagy (3rd edition). *Autophagy* **12**, 1–222 (2016).
34. Tabara, L. C. & Escalante, R. VMP1 establishes ER-microdomains that regulate membrane contact sites and autophagy. *PLoS ONE* **11**, e0166499 (2016).
35. Czabotar, P. E., Lessene, G., Strasser, A. & Adams, J. M. Control of apoptosis by the BCL-2 protein family: implications for physiology and therapy. *Nat. Rev. Mol. Cell Biol.* **15**, 49–63 (2014).
36. Molejon, M. I., Ropolo, A., Re, A. L., Boggio, V. & Vaccaro, M. I. The VMP1-Beclin 1 interaction regulates autophagy induction. *Sci. Rep.* **3**, 1055 (2013).
37. Chiang, W. C. et al. High-throughput screens to identify autophagy inducers that function by disrupting Beclin 1/Bcl-2 binding. *ACS Chem. Biol.* **13**, 2247–2260 (2018).
38. Bodo, J. et al. Acquired resistance to venetoclax (ABT-199) in t(14;18) positive lymphoma cells. *Oncotarget* **7**, 70000–70010 (2016).
39. Kotschy, A. et al. The MCL1 inhibitor S63845 is tolerable and effective in diverse cancer models. *Nature* **538**, 477–482 (2016).
40. Zheng, L., Chen, L., Zhang, X., Zhan, J. & Chen, J. TMEM49-related apoptosis and metastasis in ovarian cancer and regulated cell death. *Mol. Cell Biochem.* **416**, 1–9 (2016).
41. Lonc, C. et al. The pancreatitis-associated protein VMP1, a key regulator of inducible autophagy, promotes Kras(G12D)-mediated pancreatic cancer initiation. *Cell Death Dis.* **7**, e2295 (2016).
42. Mortensen, M. et al. The autophagy protein Atg7 is essential for hematopoietic stem cell maintenance. *J. Exp. Med.* **208**, 455–467 (2011).
43. Stephenson, L. M. et al. Identification of Atg5-dependent transcriptional changes and increases in mitochondrial mass in Atg5-deficient T lymphocytes. *Autophagy* **5**, 625–635 (2009).
44. Liang, C. C., Wang, C., Peng, X., Gan, B. & Guan, J. L. Neural-specific deletion of FIP200 leads to cerebellar degeneration caused by increased neuronal death and axon degeneration. *J. Biol. Chem.* **285**, 3499–3509 (2010).
45. Bellot, G. et al. Hypoxia-induced autophagy is mediated through hypoxia-inducible factor induction of BNIP3 and BNIP3L via their BH3 domains. *Mol. Cell Biol.* **29**, 2570–2581 (2009).
46. Rodriguez, M. E., Catrinacio, C., Ropolo, A., Rivarola, V. A. & Vaccaro, M. I. A novel HIF-1alpha/VMP1-autophagic pathway induces resistance to photodynamic therapy in colon cancer cells. *Photochem. Photobiol. Sci.* **16**, 1631–1642 (2017).
47. Valentin, R., Grabow, S. & Davids, M. S. The rise of apoptosis: targeting apoptosis in hematologic malignancies. *Blood* **132**, 1248–1264 (2018).
48. Bosman, M. C. et al. The TAK1-NF-kappaB axis as therapeutic target for AML. *Blood* **124**, 3130–3140 (2014).
49. Jilg, S. et al. Blockade of BCL-2 proteins efficiently induces apoptosis in progenitor cells of high-risk myelodysplastic syndromes patients. *Leukemia* **30**, 112–123 (2016).
50. Mehta, S. V., Shukla, S. N. & Vora, H. H. Overexpression of Bcl2 protein predicts chemoresistance in acute myeloid leukemia: its correlation with FLT3. *Neoplasma* **60**, 666–675 (2013).
51. Liu, B. et al. Venetoclax and low-dose cytarabine induced complete remission in a patient with high-risk acute myeloid leukemia: a case report. *Front. Med.* **12**, 593–599 (2018).
52. Pan, R. et al. Selective BCL-2 inhibition by ABT-199 causes on-target cell death in acute myeloid leukemia. *Cancer Discov.* **4**, 362–375 (2014).
53. Konopleva, M. et al. Efficacy and biological correlates of response in a phase II study of venetoclax monotherapy in patients with acute myelogenous leukemia. *Cancer Discov.* **6**, 1106–1117 (2016).
54. Sriskanthadevan, S. et al. AML cells have low spare reserve capacity in their respiratory chain that renders them susceptible to oxidative metabolic stress. *Blood* **125**, 2120–2130 (2015).
55. Marquez-Jurado, S. et al. Mitochondrial levels determine variability in cell death by modulating apoptotic gene expression. *Nat Commun* **9**, 389 (2018).